Generation of DC-Driven Non-Thermal Plasma in Atmospheric Pressure Air

J. Choi, T. Namihira, S. Katsuki and H. Akiyama

Graduate School of Science and Technology, Kumamoto University. Kurokami 2-39-1, Kumamoto city, Kumamoto 860-8555, Japan

The main advantage of atmospheric pressure plasma processing is that it requires much lower investment costs, because no vacuum devices are needed, in the case of ambient air, not even a housing. From these points of view, a dc-driven atmospheric pressure air plasma generator, which is pen-type, has been developed in this paper. The main experimental results are as follows. The discharge occurred periodically in spite of dc input. The length of the plasma torch depended on the tube diameter and it was saturated around the flow rate of 2 l/min. The spatial distributions of plasma gas temperature were measured with an electromagnetically proof thermometer, and confirmed by the visualization of gas flow using Schlieren images. Furthermore, surface treatment and decolorization using the generated plasma torch were carried out aiming at industrial applications.

1. Introduction

Non-thermal atmospheric pressure plasmas have been successfully implemented for various industrial applications such as material processing, surface treatment, biochemical decontamination, gas combustion, and laser excitation [1-10]. The main advantage of atmospheric pressure plasma processing is that it requires much lower investment costs, because no vacuum devices are needed, in the case of ambient air, not even a housing. Hence, the implementation of devices into assembly lines with renouncement of batch procedures is greatly facilitated. Also, the majority of atmospheric plasmas are easily scaled up.

From these points of view, a dc-driven atmospheric pressure air plasma generator [11], which is pen-type, has been developed in this paper. Also, various physical properties such as torch lengths, the spatial distributions of gas temperature, the visualization of gas streams, wettability, and ozone yield are investigated.

2. Experimental Setup

Figure 1 shows the schematic diagram of the experimental set-up used in this study. A tungsten (W) needle electrode (0.2 mm diameter) is placed in a glass tube (mostly 0.6 mm i.d., 1.0 mm o.d.), and a copper (Cu) plane electrode with a hole (1.6 mm diameter in case of 0.6 mm i.d.) is placed at the nozzle of the tube end. The gap distance between the electrodes is 2mm. The electric arc is formed between the electrodes by applying HV dc power through a blocking resistor, R_1. By introducing dry air into the tube, the plasma gas of the arc is spewed out from the nozzle, and a plasma torch is generated at atmospheric pressure. The applied voltage between the electrodes and the arc current have been measured using a voltage divider (EP-50K, Pulse Electronic Engineering Co., Japan) and a non-inductive resistor (R_2, 100 Ω), respectively. An oscilloscope (TDS3054B, 500 MHz, Tektronix) recorded the single-shot signals from the measuring devices.

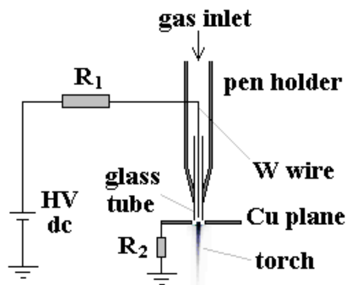

Fig. 1. Schematic diagram of the experimental set-up

3. Results and Discussion

Figure 2 shows the typical voltage and current waveforms between the electrodes. From the figure, it can be seen that the discharge is periodically occurring in spite of dc input and that the current pulse width is very short (about 20 ns). Actually, the plasma is found to be self-pulsing. Therefore, very low power consumption in the discharge is expected. The repetition rate of the current pulses increases with the input power.

Figure 3 shows the plasma torch taken with the hand-held digital camera. The arc column between the electrodes forms the shape of J or U by the gas flow. Simultaneously, the plasma gas of the arc is spewed out from the nozzle with the velocity of the gas flow (0.1 l/min – 5.0 l/min).

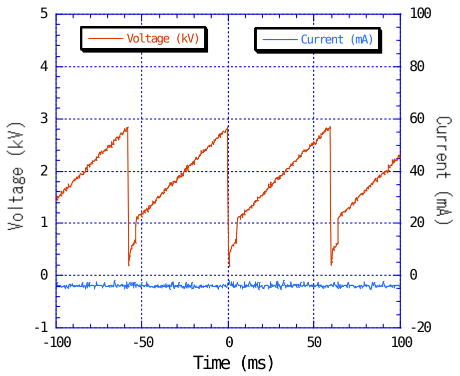

(a) Focused on the periodic voltage waveform (50ms/div)

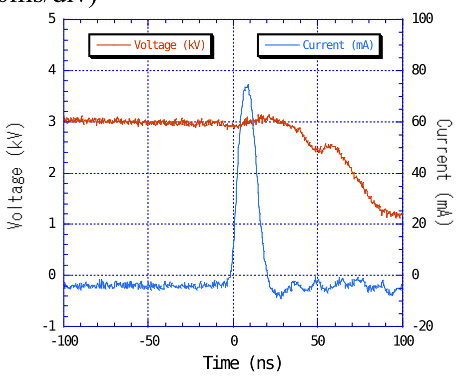

(b) Focused on the current pulse waveform (50 ns/div)

Fig. 2. Typical voltage and current waveforms

Fig. 3. Photograph of the generated micro-plasma torch (nozzle i.d.: 0.6 mm)

The visible torch length was measured as a function of the gas flow rate with the naked eye in a dark room, as shown in Figure 4. The torch length increases with the flow rate up to about 2 l/min, and then reaches saturation. The mechanism of the saturation is not understood at present. In addition, it was found that the torch length increases with the diameter of the glass tube although it is thought that the length is influenced in part by the different input power.

Figure 5 shows the axial distributions of the gas temperature from the nozzle, which were measured with a fluorescence thermometer (FL-2000, Anritsu Meter Co., Japan) that is electro- magnetically proof. The plasma temperature has a maximum in the vicinity of the nozzle, and drastically decreases to the distance of 10 cm from the nozzle.

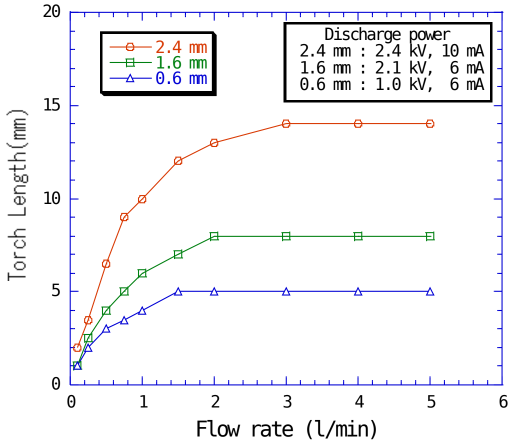

Fig. 4. Dependence of visible torch length on flow rate

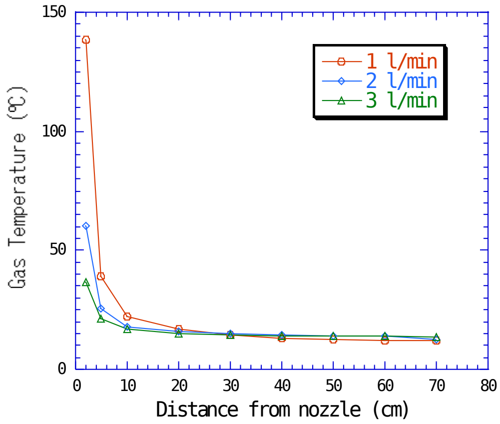

Fig. 5. Axial distribution of gas temperature in the gas column (nozzle i.d.: 0.6 mm, ambient temperature: 13.5 at 0 cm, 11.9 at 70 cm)

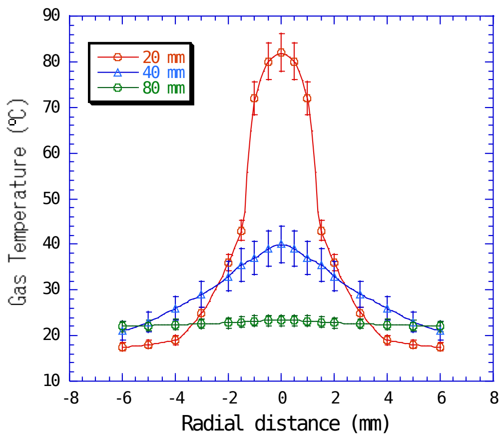

Fig. 6. Radial distribution of gas temperature in the gas column (nozzle i.d.: 0.6 mm, flow rate: 1.5 l/min)

It should be noted that, in the near area inside 30 cm from the nozzle, the gas temperature in the case of 1 l/min is higher than that in the case of 3 l/min and that, in the far area over 30 cm, the situation is reversed. This is attributed to both gas velocity and cooling effect of the gas flow.

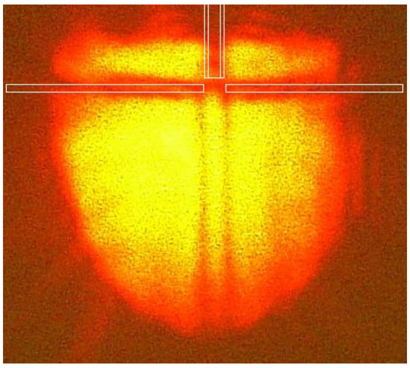

(a) 0 mm from the nozzle

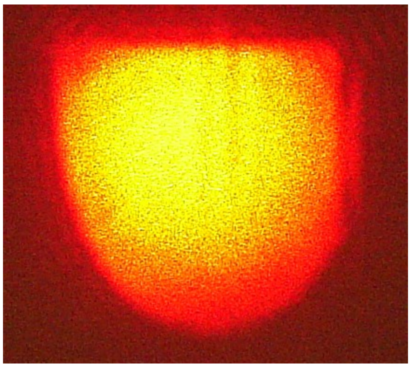

(b) 30 mm down from the nozzle

Fig. 7. Schlieren images of gas stream (nozzle i.d.: 0.6 mm, flow rate: 1.5 l/min, pinhole i.d.: 100 μm, lens focus: 15 cm)

Figure 6 shows the radial distributions of the gas temperature from the torch axis, which were measured at the distance of 20 mm, 40 mm and 80 mm from the nozzle respectively. From the figure, it can be seen that the temperature gradient is very steep in the case of 20 mm, whose full width at half maximum (FWHM) is about 2.5 mm, and that the flatness of the distribution increases with the distance from the nozzle.

In order to make sure of the spatial distribution of the plasma torch as shown in Figure 5 and Figure 6, Schlieren images of the gas flow were taken using a He/Ne laser. The results are shown in Figure 7. From Figure 7 (a), it can be seen that the gas flow is clearly visualized due to the different density from the ambient air. The width of the gas column remains to be shorter than 2 mm even until it disappears around 40 mm from the nozzle as shown in Figure 7 (b). It appears that the visualized gas column consists of mainly warm gas flow from the fact that the configuration of the Schlieren image is quite different from that of the visible plasma torch as shown in Figure 3, which appears to consist of mainly excited species. The lowest temperature to be visualized on the Schlieren image can be derived as about 36 referring to the temperature for the same width in the case of 40 mm in Figure 6.

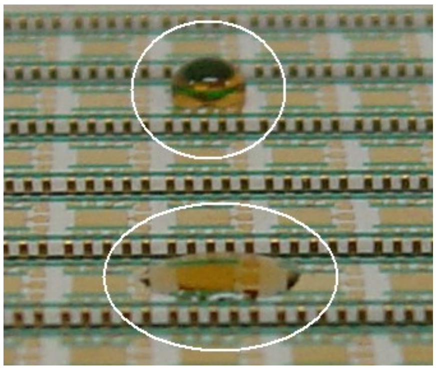

Fig. 8. Photograph of water droplets on PCB. Top: untreated surface, Bottom: treated surface (exposed time: 10 sec, Gap: 5 mm, water-droplet: 5 μl)

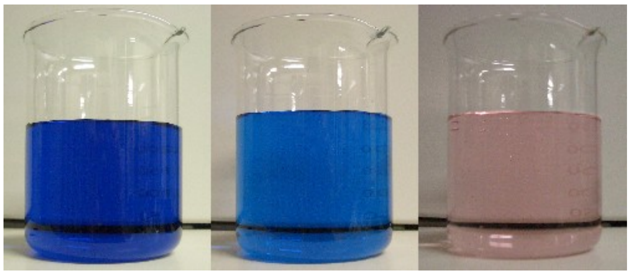

(a) 0 minutes (b) 60 minutes (c) 90 minutes

Fig. 9. Decolorization of Indigo Carmine (25 mg/l, nozzle i.d.: 1.6 mm, flow rate: 2 l/min)

Figure 8 shows the effect of the surface treatment using the generated torch plasma on a PCB, of which manufacturer has ordered the authors to modify the hydrophilic property of the PCB. The droplet on the untreated surface takes a semi-spherical form, whereas that on the treated surface spread out almost flat. Thus, drastically reduced contact-angle (>90°) can be obtained from this result. In order to verify the role of the radicals in the plasma torch in wettability improvement, hot gas of the same treatment temperature from a commercial dryer was applied to the PCB, resulting in no modification.

Figure 9 shows the effect of the decolorization for Indigo-dissolved water (Indigo Carmine ($C_{16}H_8N_2Na_2O_8S_2$=466.35): Nacalai Tesque Inc. Japan). It took a relatively long treatment time because of low ozone yield (16 mg/m^3 for 10 mA, 120 mg/m^3 for 20 mA) measured with a UV spectrophotometer (model V-550, JASCO Corp. Japan). On the other hand, underwater operation of the plasma torch was also confirmed.

4. Conclusions

Making the best use of the merits of plasma generation in atmospheric pressure air, a dc-driven capillary plasma generator, which is pen-type, has been developed. The discharge occurred periodically in spite of dc input. The plasma torch length depended on the tube diameter and it was saturated around the flow rate of 2 l/min. The spatial distributions of plasma gas temperature were measured with an electromagnetically proof thermometer, and confirmed by the visualization of gas flow using Schlieren images. Furthermore, surface treatment and decolorization using the generated plasma torch were carried out aiming at industrial applications.

5. References

[1] H. U. Poll, M. Artz and K. H. Wickleder, *Eur. Polym. J.*, 12305 (1976).

[2] J. W. Coburn, *IEEE Trans. Plasma Sci.*, Vol. 19, No. 6 (1991) 1048-1062.

[3] R. Dorai and M. Kushner, *J. Phys. D: Appl. Phys.* 36 (2003) 666-685.

[4] K. Tanaka, T, Inomata and M. Kogoma, *Plasma and Polymers* 4 (1999) 269-281.

[5] B. Eliasson and U. Kogelschatz, *IEEE Trans. Plasma Sci.*, Vol. 19, No. 6 (1991) 1063-1077.

[6] V. Karanassios, *Spectrochimica Acta* Part B 59 (2004) pp. 909-928.

[7] J. Hopwood, F. Iza, S.Coy and D. B. Fenner, *J. Phys. D: Appl. Phys.* 38 (2005) 1698-1703.

[8] M. Laroussi, *IEEE Trans. Plasma Sci.*, Vol. 30, No. 4 (2002) 1409-1415.

[9] T. Wagner, W. O'Brien, G. Northam and J. Eggers, *J. Propulsion and Power* 5 (1989) 5.

[10] I. Hayashi, *High voltage Plasma Engineering* (in Japanese) (1996)

[11] Private communications with Prof. Karl H. Schoenbach (Old Dominion University, USA).